ChemPubSoc Europe

DOI: 10.1002/chem.201502303

CHEMISTRY A European Journal Full Paper

Nanotechnology |*Hot Paper*|

Single-Step Exfoliation and Covalent Functionalization of MoS_2 Nanosheets by an Organosulfur Reaction

Ricardo H. Gonçalves,*[a] Rodrigo Fiel,[a] Mario R. S. Soares,[a] Wido H. Schreiner,[b] Caio M. P. Silva,[a] and Edson R. Leite*[a]

Abstract: A simple approach to exfoliate and functionalize MoS_2 in a single-step is described, which combines the dispersion of MoS_2 in polybutadiene solution and ultrasonication processes. The great advantage of this process is that a colloidal stability of MoS_2 in nonpolar solvent is achieved by chemically bonding polybutadiene on the perimeter edge sites of MoS_2 sheets. In addition, elastomeric nanocomposite has been prepared with singular mechanical properties using functionalized MoS_2 as nanofiller in a polybutadiene matrix with a subsequent vulcanization reaction.

Introduction

Two-dimensional materials, such as molybdenum disulfide (MoS_2), have been extensively studied due to their applicability in different areas, such as catalysis, electrocatalysis, and electronic devices.[1–8] Furthermore, recent reports have demonstrated that 2D-MoS_2 has a high Young's modulus, for example, 270 GPa.[9–13] This impressive mechanical property associated with sheet morphology makes the 2D-MoS_2 a candidate for application as a nanofiller with polymeric composites. However, the use of 2D-MoS_2 for the development of polymeric composites demands a large amount of this material, which can be obtained through methods of exfoliation, such as chemical exfoliation by lithium intercalation[14–17] and mechanical exfoliation by ultrasonication with the affinity solvent.[18–24] Mechanical exfoliation can be assisted by an adsorbed polymer and the use of soluble polymer chains during the process, allowing exfoliated 2D materials to be obtained in solvents that could not otherwise exfoliate successfully.[25,26] Basically, the polymer chains attached to the nanosheets promote its colloidal stabilization against aggregation. The polymeric chains can be attached either by covalent bonds (grafted) or by van der Waals (vdW) forces.[26] Mechanical exfoliation assisted by an adsorbed polymer opens pathways for the development of new composite materials, including the development of composites with nonpolar polymer matrices as the polyolefins and polybutadiene (PB) elastomers.

Besides, the lamellar structure of the 2H-MoS_2 with van der Waals interactions between S–Mo–S slabs and alternative edge terminations[27,28] allows the development of composites with selective reinforcement. For instance, it is possible to increase the elastic modulus of the composite by using noncovalent polar interactions between the polymer matrix and the basal plane of the 2D-MoS_2, or to promote the interaction between the 2D-MoS_2 edges and the polymer matrix through a suitable selective functionalization.[29,30] Theoretical studies, using DFT, suggest the edge sites of the MoS_2 possess high molecular affinity.[31] Recently, Chou et al. showed that it is possible to modify the internal and perimeter edges of 2D-MoS_2 using thiol ligand functionalization.[32]

Based on these promising perspectives of the 2D-MoS_2 for the development of novel nanocomposites,[33–35] we developed a process that, in a single step, aids the mechanical exfoliation of the MoS_2 by ultrasonication assisted by an adsorbed polymer and inducing the chemical bonding of the polymeric chain to the MoS_2 sheets. The terminal sulfur located in the edge sites of the 2D-MoS_2 bind selectively onto the PB chain through an organosulfur reaction, resulting in a molecular nanocomposite. We also showed an application of these grafted 2D nanofillers in elastomeric nanocomposites by solution-based processing.

Results and Discussion

In a typical experiment, the MoS_2 powder is sonicated in a toluene/*N*-methyl-2-pyrrolidone (NMP) mixture and in PB dissolved in toluene/NMP for over six days (see details in the Experimental Section). The MoS_2 sonicated in polymer solution shows very high colloidal stability, as can be seen Figure 1a. Moreover, the poor colloidal stability of the MoS_2, without PB, sonicated in toluene/NMP suggests a lower degree of exfoliation (see Figure 1a and Figure S3b, Supporting Information). The

[a] *R. H. Gonçalves, R. Fiel, M. R. S. Soares, Prof. Dr. C. M. P. Silva, Prof. Dr. E. R. Leite*
Department of Chemistry
Federal University of Sao Carlos, Sao Carlos, SP, Brazil
E-mail: ricardohg.ufscar@gmail.com
edson.leite@pq.cnpq.br

[b] *Prof. Dr. W. H. Schreiner*
Department of Physics
Federal University of Paraná, Curitiba PR, Brazil

Supporting information and ORCID(s) from the author(s) for this article are available on the WWW under http://dx.doi.org/10.1002/chem.201502303.

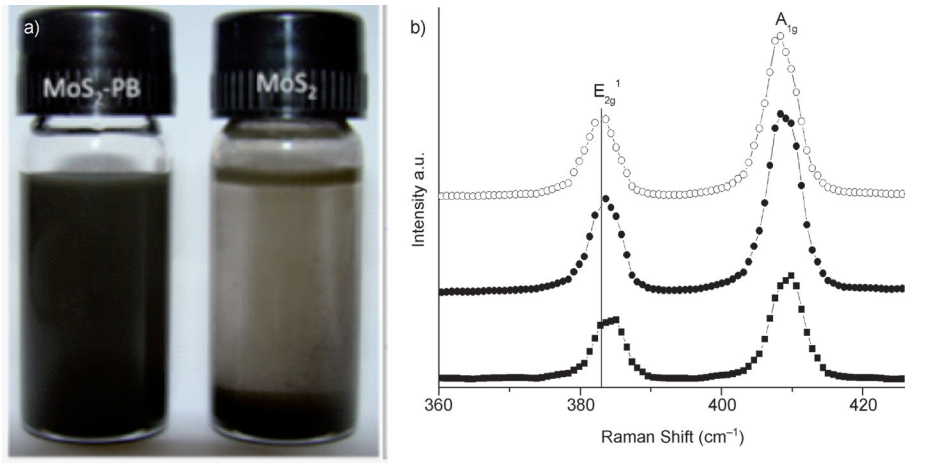

Figure 1. a) Photograph of vials showing colloidal stability of MoS_2-PB and MoS_2 dispersed in pure toluene. b) Raman spectroscopy analysis of bulk MoS_2 (○), MoS_2 sonicated in toluene/NMP (●) and MoS_2 sonicated in a PB polymer solution (■).

exfoliation state of material sonicated in polymer solution was characterized by Raman spectroscopy and TEM. Under these conditions, the Raman spectroscopy analysis of bulk MoS_2 (Figure 1 b), shows two characteristic Raman modes, E^1_g (383.2 cm^{-1}) and A_{1g} (409.7 cm^{-1}), with a frequency difference of 26.5 cm^{-1}, as expected for a nonexfoliated material. After sonication in polymer solution, the material shows Raman peaks at 384.2 and 409.3 cm^{-1}, for the E^1_g and A_{1g} Raman modes respectively, with a frequency difference of 25.1 cm^{-1}. This shift in the Raman modes indicates a high degree of exfoliation, resulting in a 2D-MoS_2 material formed by a few layers (~4–6 layers).[35–37] The high degree of exfoliation is confirmed by the AFM measurements (see Figure S1 in the Supporting Information). The AFM image clearly shows MoS_2 sheets with dimensions of micrometers and height of a few nanometers. The line profile analysis indicated (see Figure S2b in the Supporting Information) a height of 3.3 nm, equivalent to five layers. The frequency difference between the E^1_g and A_{1g} Raman modes for the materials sonicated in pure toluene/NMP is very similar to the value measured for the bulk MoS_2, confirming the low degree of exfoliation of the MoS_2 sonicated in the solvent mixture without the PB addition.

Figure 2 a shows a HRTEM image of MoS_2 exfoliated in PB solution. The representative TEM image shows several flakes with sheet morphology and lateral dimensions ranging from 100 to 700 nm. In addition, most of the flakes were electron transparent, indicating a high degree of exfoliation (see more TEM images in Figure S2, Supporting Information). The TEM analysis is in agreement with the Raman spectroscopy results, which indicate that the exfoliation process performed in PB-toluene/NMP solution is effective for processing 2D-MoS_2 materials.

The chemical interaction between the PB chains and MoS_2 was studied by XPS analysis. In Figure 3 a, the XPS spectrum for the MoS_2-PB shows two peaks at 229.1 and 232.0 eV, which correspond to Mo^{4+} $3d_{5/2}$ and Mo^{4+} $3d_{3/2}$, respectively. This analysis confirms no formation of molybdenum oxide on the edge of MoS_2. S2p peaks at 161.7 and 162.9 eV were also observed (Figure 3 b). To evaluate the chemical interaction between the PB and the exfoliated MoS_2, we analyzed the carbon C1s peak. Figure 3 c–d show the XPS spectra for the exfoliated MoS_2 in PB solution and pure PB respectively. The C1s peak analysis of the pure PB (Figure 3 d) shows peaks related to C=C, C-C and C–H bonds, as expected. On the other hand, the C1 s peak analysis of the exfoliated MoS_2 in PB solution (Figure 3 c) shows a complex set of C1s peaks. After a deconvolution process, using the Gaussian function, it was able to identify at 286.6 and 288.7 eV, C–C–S and C–S bonds,

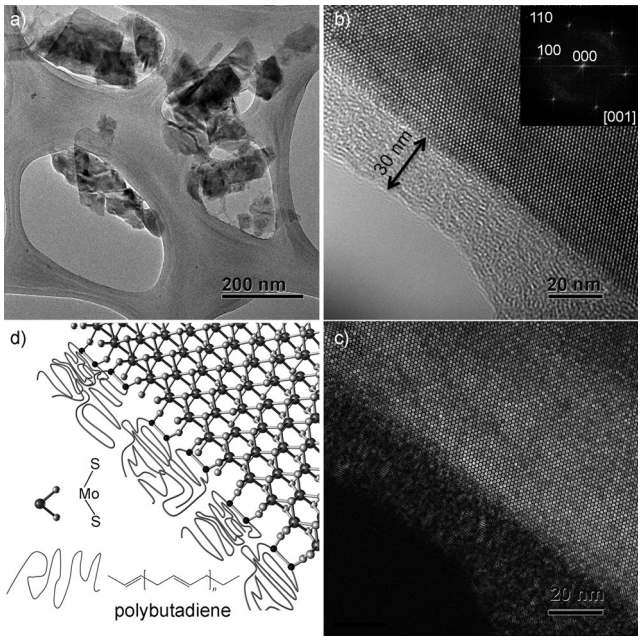

Figure 2. TEM images of MoS_2 covalently functionalized with polybutadiene. a) Low magnification TEM image b) Polybutadiene layer on the MoS_2 edge. c) Image filtered by Sobel operator to enhance the polymer and HRTEM image. d) Scheme of polymeric chains bonded on the MoS_2.

respectively,[38–39] which suggests the chemical reaction between the PB and MoS_2 nanosheets. The carbidic carbon residue was also observed in XPS analysis at 282.7 eV. This residual carbon is due to molybdenum carbon in the synthetic process of MoS_2 powder.[40,41]

Moreover, the HRTEM image in Figure 2 b shows MoS_2 sheets oriented along the [001] zone axis (see Figure 2 b inset showing FFT analysis) with a well-defined polymer layer located rather at the perimeter edges of the sheets. Figure 2 d shows the HRTEM image of Figure 2 b after the Sobel operator filter has been applied, aiming to enhance the contrast be-

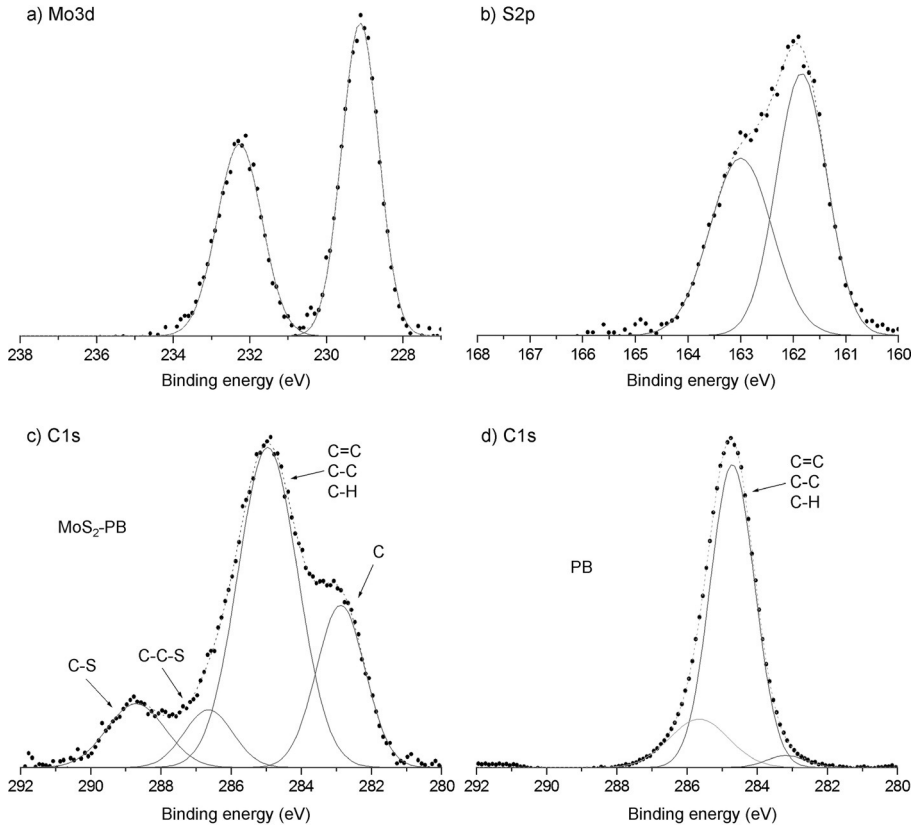

Figure 3. XPS spectra of PB anchored on the MoS_2 nanosheets. a) Mo3d peaks and b) S2p peaks for MoS_2-PB. c) C1s XPS analysis for the MoS_2-PB and d) C1s only PB pure.

tween the PB chain and the MoS_2 edge sites. A very good interface can be seen between the polymer and the exfoliated MoS_2. The HRTEM analysis indicates a preferential bond between the PB and 2D-MoS_2 at the perimeter edges of the sheets. The preferential PB bonding at the 2D-MoS_2 perimeter edges of the sheets is confirmed by the AFM analysis (see Figure S1a in the Supporting Information). In this AFM image, we can notice polymers bonded only in the border of the Mos_2 sheets. A plausible explanation for the identification of C–S bond and the formation of a polymer layer around the MoS_2 sheets is the reaction between the C=C of the PB chains and the terminal sulfur of the MoS_2 nanosheets through a covalent bond, as illustrated in Figure 2c.

The FTIR spectroscopic analysis (see Figure S3, Supporting Information) also showed the presence of PB bounded on the MoS_2 surface. The modifications in the bands at 3070 cm^{-1} (depict C=C–H stretch) 1667 cm^{-1} (relative to C=C stretch) and in 630 cm^{-1} (which is attributed to a C–S stretch) confirm the chemical interaction between the PB and the 2D-MoS_2. The FTIR spectrum of MoS_2-PB supports the result obtained in the XPS analysis.

The PXRD, in Figure 4a, shows only one peak corresponding to the plane (002) for the MoS_2 exfoliated in PB solution. The PXRD pattern also shows broad (002) peak that confirms the reduction of the initial size of the MoS_2 to nanoscale size. The presence of the single peak (002) in the PXRD is due to the restacking of the functionalized MoS_2 sheets on the substrate.[42] This restacked MoS_2 has been frequently reported in process involving lithium intercalation.[43] The PXRD for the MoS_2 exfoliated only in toluene/NMP (without PB) showed all characteristic crystallographic peaks of bulk MoS_2, as can be seen in Figure 4a (black line), confirming the low degree of exfoliation. The thermogravimetric analysis (TGA) also allowed quantifying the amount of PB anchored on the MoS_2, as illustrated in Figure 4b. A weight loss of 8.5% is reported and we associated this weight loss to the total amount of PB. The TGA also was performed in inert atmosphere to avoid the formation of molybdenum oxide. The weight loss calculated was 6.1% (see Figure S4, Supporting Information). This difference compared with the result obtained in synthetic air is correlated with solid residue formed from PB, during the thermal decomposition.

As described above, the exfoliation process in a PB/toluene solution allowed a grafted 2D-MoS_2 with the polymer chains bonded at the perimeter edges of the sheets to be obtained. Evidently, the preferential location of the PB around the sheets suggests a poor interaction of the polymer chains with the basal planes of the MoS_2. Thus, this grafted nanofiller can lead to the development of a nanocomposite with controlled reinforcement. To demonstrate this hypothesis, we decided to incorporate the nanofiller in a very simple elastomeric formulation, using PB as a polymeric matrix. As described in the Experimental Section, the composite material was prepared by solution processing and the reticulation process was promoted by sulfur addition only. Generally, some additives, such as zinc oxide, carbon black, and plasticizers are added in PB rubber formulation to increase the stretch and strain modulus of the rubber. However, in this instance, these kinds of additives were not used in order to evaluate the effect of the PB grafted 2D-MoS_2 on the mechanical properties of the nanocomposite. During the composite preparation, all vulcanization parameters were kept constant, such as temperature, time, and sulfur amount. For this study only the amount of the nanofiller was modified.

Figure 5 shows the cross-sectional SEM images of the nanocomposite and PB vulcanized elastomer. As revealed in Figure 5a, a homogeneous dispersion of PB-grafted 2D-MoS_2 nanosheets on the PB matrix is observed, even for a concentration of 30 wt% of the nanofiller. This observation confirms the excellent chemical compatibility between the nanofiller and

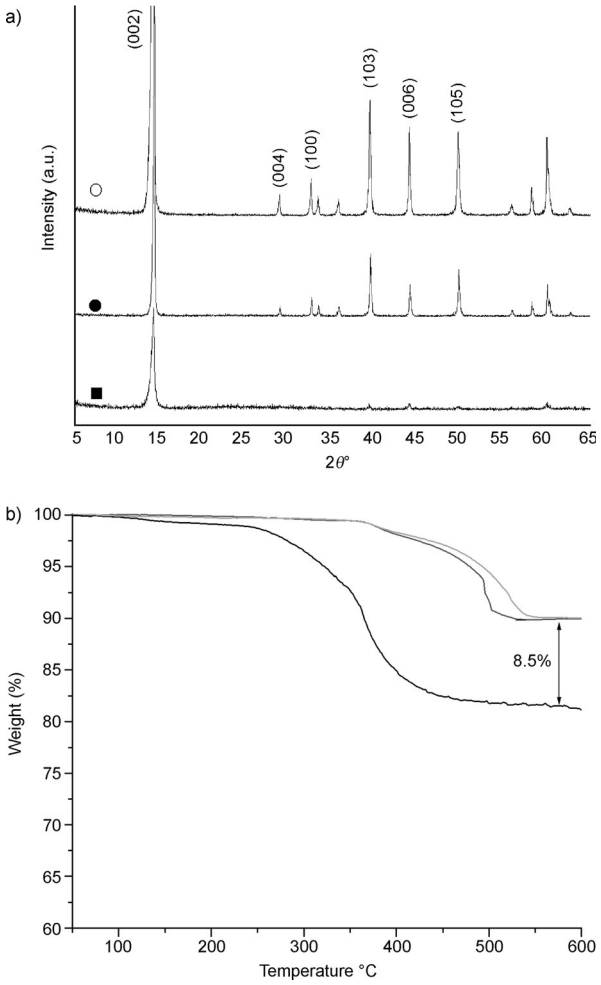

Figure 4. a) PXRD pattern for the MoS_2 exfoliated in PB solution (■), only toluene/NMP solution (●), and bulk MoS_2 (○). b) Thermogravimetric analysis performed in synthetic air (bulk MoS_2: ——; MoS_2 sonicated in toluene/NMP: ——; MoS_2 sonicated in a PB solution: ——).

the polymer matrix. Figure 5b shows the SEM image of pure PB vulcanized. The nanocomposite material prepared with different PB grafted 2D-MoS_2 loading was mechanically characterized by tensile testing. Figure 6a shows representative stress–strain curves for composites filled with loading levels ranging from 0 to 30 wt%. It is interesting to observe that the addition of the MoS_2 nanofiller promotes a significant modification in the mechanical behavior of the PB vulcanized rubber. With exception of the sample with 30 wt% of nanofiller, it is evident, from the stress–strain curves, the addition of the PB-grafted 2D-MoS_2 promotes a decrease of the Young's modulus and tensile strength and an increase in the strain (see Figure 5b).

It is well known that the tensile strength of vulcanized elastomers largely depends on the ability of the polymeric chain to untangle and align when a stretching force is applied. The reduction of the tensile strength with the addition of a nanofiller suggests that the filler is acting as a solid lubricant of the PB chains. However, when we increased the filler loading, the alignment of the MoS_2 sheets starts to control the mechanical behavior of the nanocomposite, increasing the tensile strength and decreasing the maximum strain. It is important to point out that by controlling the filler content, it was possible to obtain a composite material with high tensile strength and high strain. For instance, the sample with 20 wt% of nanofiller shows a tensile strength similar to the pure PB elastomer. However, there was a strain improvement by more than threefold. The unusual mechanical behavior described before must be a direct consequence of the PB polymer chains bonded at the perimeter edges of the MoS_2 sheets and the poor interaction between the nonpolar polymer chain with the basal (001) plane of the MoS_2.

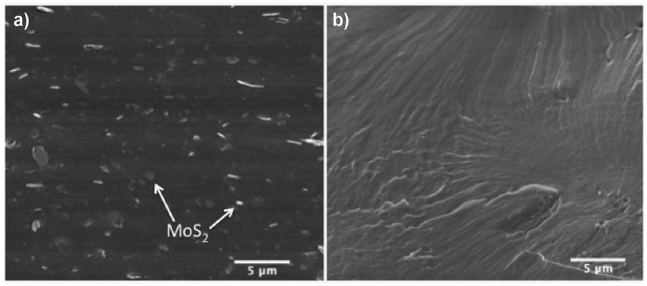

Figure 5. SEM images of molecular elastomeric nanocomposite with different concentrations of MoS_2-PB. a) Substantial amounts of 30 wt% MoS_2 sheets in PB. b) Pure polybutadine vulcanized.

Conclusion

In summary, our experimental studies yield a novel approach to produce, in a single step, the exfoliation and functionalization of MoS_2. We demonstrated that exfoliation process in a PB/toluene solution allowed obtaining a grafted 2D-MoS_2 with the PB polymer chains bonded at the perimeter edges of the sheets. The grafted 2D-MoS_2 is considered here a molecular nanocomposite. This grafted 2D nanofiller creates possibilities to introduce new functionality to the MoS_2 sheets. For instance, the use of this nanofiller to modify the mechanical behavior of a vulcanized PB elastomer observed unusual mechanical behavior as function of filler concentration, which must be related to preferential locations of the PB chains at the perimeter edges of the MoS_2 sheets and the poor interaction between

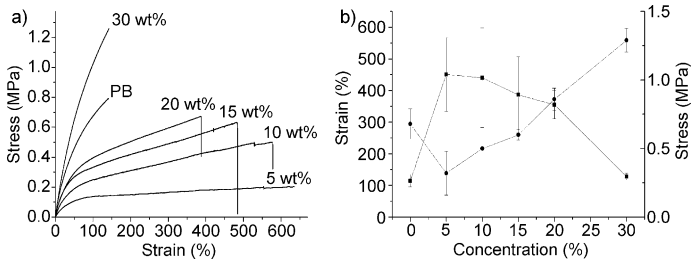

Figure 6. Mechanical measurement of molecular nanocomposite. a) Stress–strain curve for different loadings of MoS_2 sheets. b) Elongation modulus versus loading concentrations.

the nonpolar polymeric chains with the basal (001) plane. The novel polymer-grafted 2D-MoS_2 nanofillers can be applied to the development of nanocomposites with a polyolefin matrix processed in an extruder machine, opening new windows of opportunities for the development of materials with superior chemical resistance and low gas permeability.

Experimental Section

Materials

The MoS_2 powder, polybutadiene $Mw = 200{,}000$ NMP and elemental sulfur were purchased from sigma Aldrich. Toluene (HPLC) was purchased from Tedia.

MoS_2 exfoliation

First, polybutadiene (20 g) was dissolved in toluene (300 mL) at 80 °C. After that, NMP (200 mL) and MoS_2 (2 g, Aldrich) was added in this polymer solution. The exfoliation process was carried out in an ultrasonic bath model Branson (model 1510). In this case, the closed bottle with MoS_2/polymer was introduced in the ultrasonic bath and kept for 6 days. After this time, the unexfoliated residual MoS_2 was centrifuged at 5000 RPM (3412 rcf). The greenish supernatant was then centrifuged at 14000 rpm for 1 h and a black solid powder was obtained. This powder was washed three times with toluene to remove the excess of PB. The washed powder was easily dispersed in toluene and the concentration was calculated to be 9 mg mL^{-1}. For a comparative experiment, the MoS_2 was also exfoliated in toluene/NMP mixture and sonicated, but without addition of PB. Since MoS_2 instantly precipitated, no centrifugation process was performed in this phase.

Molecular nanocomposite

Initially, the polybutadiene (3.0 g) was solubilized in toluene (40 mL) at 80 °C. After that, elemental sulfur (0.3 g) was solubilized in the polymer solution that corresponds to 10 wt% of sulfur in 100% of polybutadiene. MoS_2 (1 wt%) was added in the transparent solution of polymer/sulfur, under stirring for one hour at 80 °C. The stable colloid (40 mL) of the MoS_2-S_8-polymer was spilled on the PTFE container and dried at 80 °C. After that, all the greenish paste was easily removed from the PTFE container. The greenish paste (2.0 g) was compressed between two PTFE sheets and vulcanized in a hot press at 150 °C for 60 min. The elastomeric polymer formed was cooled at room temperature and cut in strips of 1×5 cm with a thickness of 1 mm. The same vulcanization process was performed for different concentrations of MoS_2 (5, 15, 20, and 30 wt%) in addition to a 100 wt% of polybutadiene whilst keeping constant time, sulfur concentration, temperature, and pressure applied.

Characterization

Micro-Raman spectrum was collected in Synapse Horiba Jobin Yvon with a Nd:YAG (wavelength of 532 nm). The single-crystal Si was used as reference in the spectrum (Raman band at 520 cm^{-1}). A TEM image was acquired with a Tecnai F-20 operating at 200 kV. The crystallographic phase of the MoS_2 nanosheets powder was determined on a Rigaku D/MAX-2500 diffractometer using $Cu_{K\alpha}$ radiation. FTIR spectra ware collected with a Bruker Equinox 55 spectrometer. TGA was performed on a Netzsch model STA 409 to determine PB chains loss under synthetic air and nitrogen gas at a heat rate of 10 °C.min^{-1}. The XPS analysis was obtained in a VG Microtech ESCA 3000 spectrometer with a base vacuum of 3.10^{-10} mbar, a 250 mm semi-hemispherical analyzer with nine channeltrons, and $Al_{K\alpha}$ nonmonochromatic radiation. For AFM characterization the MoS_2-PB was deposited onto a flashly cleaved mica substrate. The measurement was performed using Nanosurf Easyscan equipment.

Acknowledgements

The financial support of FAPESP (Proc. 2013/02468-0), CNPq, and CAPES (all Brazilian agencies) is gratefully acknowledged.

Keywords: covalent functionalization · exfoliation · MoS_2 nanosheets · nanocomposites · organosulfur

[1] P. Joensen, R. F. Frindt, S. R. Morrison, *Mater. Res. Bull.* **1986**, *21*, 457.
[2] T. Y. Park, I.-S. Nam, Y. G. Kim, *Catalyst Ind. Eng. Chem. Res.* **1997**, *36*, 5246.
[3] M. Del Valle, J. Cruz-Reyes, M. Avalos-Borja, S. Fuentes, *Catal. Lett.* **1998**, *54*, 59.
[4] C. T. Tye, K. J. Smith, *Top. Catal.* **2006**, *37*, 129.
[5] T. F. Jaramillo, K. P. Jørgensen, J. Bonde, J. H. Nielsen, S. Horch, I. Chorkendorff, *Science* **2007**, *317*, 100.
[6] A. B. Laursen, S. Kegnæs, S. Dahl, I. Chorkendorff, *Energy Environ. Sci.* **2012**, *5*, 5577.
[7] M. A. Lukowski, A. S. Daniel, F. Meng, A. Forticaux, L. Li, S. Jin, *J. Am. Chem. Soc.* **2013**, *135*, 10274.
[8] X. Huang, C. L. Tan, Z. Y. Yin, H. Zhang, *Adv. Mater.* **2014**, *26*, 2185.
[9] I. Kaplan-Ashiri, S. R. Cohen, K. Gartsman, R. Rosentsveig, G. Seifert, R. Tenne, *J. Mater. Res.* **2004**, *19*, 454.
[10] J. Feldman, *J Phys Chem. Solids* **1976**, *37*, 1141.
[11] S. Bertolazzi, J. Brivio, A. Kis, *ACS Nano* **2011**, *5*, 9703.
[12] A. Castellanos-Gomez, M. Poot, G. A. Steele, H. S. J. van der Zant, N. Agrait, G. Rubio-Bollinger, *Adv. Mater.* **2012**, *24*, 772.
[13] A. Kis, D. Mihailovic, M. Remskar, A. Mrzel, A. Jesih, I. Piwonski, A. J. Kulik, W. Benoi, L. Forro, *Adv. Mater.* **2003**, *15*, 733.
[14] J. N. Coleman, M. Lotya, A. O'Neill, S. D. Bergin, P. J. King, U. Khan, K. Young, A. Gaucher, S. De, R. J. Smith, *Science* **2011**, *331*, 568.
[15] J. Zheng, H. Zhang, S. Dong, Y. Liu, C. Tai Nai, H. Suk Shin, H. Young Jeong, B. Liu, K. Ping Loh, *Nat. Commun.* **2014**, *5*, 2995.
[16] R. J. Smith, P. J. King, M; Lotya, C. Wirtz, U. Khan, S. De, A. O'Neill, G. S. Duesberg, J. C. Grunlan, G. Moriarty, J. Chen, J. Wang, A. I. Minett, V. Nicolosi, J. N. Coleman, *Adv. Mater.* **2011**, *23*, 3944; Lotya, C. Wirtz, U. Khan, S. De, A. O'Neill, G. S. Duesberg, J. C. Grunlan, G. Moriarty, J. Chen, J. Wang, A. I. Minett, V. Nicolosi, J. N. Coleman, *Adv. Mater.* **2011**, *23*, 3944.
[17] Z. Zeng, Z. Yin, X. Huang, H. Li, Q. He, G. Lu, F. Boey, H. Zhang, *Angew. Chem. Int. Ed.* **2011**, *50*, 11093 – 11097; *Angew. Chem.* **2011**, *123*, 11289 – 11293.
[18] Y.-H. Lee, X.-Q. Zhang, W. Zhang, M.-T. Chang, C.-T. Lin, K.-D. Chang, Y.-C. Yu, J. T.-W. Wang, C.-S. Chang, L.-J. Li, T.-W. Lin, *Adv. Mater.* **2012**, *24*, 2320.
[19] J. Q. Liu, Z. Y. Zeng, X. H. Cao, G. Lu, L. H. Wang, Q. L. Fan, W. Huang, H. Zhang, *Small* **2012**, *8*, 3517.
[20] M. Chhowalla, H. S. Shin, G. Eda, L.-J. Li, K. P. Loh, H. Zhang, *Nat. Chem.* **2013**, *5*, 263.
[21] H. Li, G. Lu, Y. L. Wang, Z. Y. Yin, C. X. Cong, Q. Y. He, L. Wang, F. Ding, T. Yu, H. Zhang, *Small* **2013**, *9*, 1974.
[22] A. O'Neill, U. Khan, J. N. Coleman, *Chem. Mater.* **2012**, *24*, 2414.
[23] K. G. Zhou, N. N. Mao, H. X. Wang, Y. Peng, H. L. Zhang, *Angew. Chem. Int. Ed.* **2011**, *50*, 10839; *Angew. Chem.* **2011**, *123*, 11031.
[24] T. Zhenghai, Q. Wei, B. Guo, *Chem. Commun.* **2014**, *50*, 3934.
[25] A. A. Jeffery, C. Nethravathi, M. Rajamathi, *J. Phys. Chem. C* **2014**, *118*, 1386.
[26] P. May, U. Khan, M. H. Hughes, J. N. Coleman, *J. Phys. Chem. A J. Phys. Chem. C.* **2012**, *116*, 11393.

[27] X. Feng, W. Xing, H. Yang, B. Yuan, L. Song, Y. Hu, K. M. Liew, *ACS Appl. Mater. Interfaces* **2015**, *7*, 13164 – 13173.
[28] R. G. Dickinson, L. Pauling, *J. Am. Chem. Soc.* **1923**, *45*, 1466.
[29] C. Ataca, S. Ciraci, *J. Phys. Chem. C* **2011**, *115*, 13303.
[30] S.-K. Kim, J. J. Wie, Q. Mahmood, H. S. Park, *Nanoscale* **2014**, *6*, 7430.
[31] P. Raybaud, J. Hafner, G. Kresse, H. Toulhoat, *Phys. Rev. Lett.* **1998**, *80*, 1481.
[32] S. S. Chou, M. De, J. Kim, S. Byun, C. Dykstra, J. Yu, J. Huang, V. P. Dravid, *J. Am. Chem. Soc.* **2013**, *135*, 4584.
[33] A. A. Gavrilov, A. V. Chertovich, P. G. Khalatur, A. R. Khokhlov, *Macromolecules* **2014**, *47*, 5400.
[34] G. Plechinger, S. Heydrich, J. Eroms, D. Weiss, C. Schuller, T. Korn, *Appl. Phys. Lett.* **2012**, *101*, 101906.
[35] X. Huang, Z. Y. Zeng, S. Y. Bao, M. F. Wang, X. Y. Qi, Z. X. Fan, H. Zhang, *Nat. Commun.* **2013**, *4*, 1444.
[36] C. Lee, H. Yan, L. E. Brus, T. F. Heinz, J. Hone, S. Ryu, *ACS Nano* **2010**, *4*, 2695.
[37] H. Li, Q. Zhang, C. C. R. Yap, B. K. Tay, T. H. T. Edwin, A. Olivier, D. Baillargeat, *Adv. Funct. Mater.* **2012**, *22*, 1385.
[38] D. G. X. Castner, *Langmuir* **1996**, *12*, 5083.
[39] H. Yu, Y. G. Jin, Z. L. Li, F. Peng, H. J. Wang, *J. Solid State Chem.* **2008**, *181*, 432.
[40] K. Oshikawa, M. Nagai, S. Omi, *J. Phys. Chem. B* **2001**, *105*, 9124.
[41] C. A. Wolden, A. Pickerell, T. Gawai, S. Parks, J. Hensley, J. D. Way, *ACS Appl. Mater. Interfaces* **2011**, *3*, 517.
[42] J. Heising, M. G. Kanatzidis, *J. Am. Chem. Soc.* **1999**, *121*, 638.
[43] G. Du, Z. Guo, S. Wang, R. Zeng, Z. Chen, H. Liu, *Chem. Commun.* **2010**, *46*, 1106.

Received: June 12, 2015
Published online on September 14, 2015